SCIENCE CHINA Materials

REVIEW

mater.scichina.com link.springer.com

Published online 4 March 2019 | https://doi.org/10.1007/s40843-018-9403-8

Sci China Mater 2019, 62(7): 913–924

Recent progress in atomic layer deposition of molybdenum disulfide: a mini review

Yazhou Huang[1,2] and Lei Liu[2*]

ABSTRACT **As a kind of specially modified chemical vapor deposition (CVD), atomic layer deposition (ALD) has long been used to fabricate thin films. The self-limiting reaction of ALD endows the films with excellent uniformity and precise controllability. The thickness of the films obtained by ALD can be controlled in an atomic scale (0.1 nm) on a large-area substrate even with complex structures. Therefore, it has recently been employed to produce the two-dimensional (2D) materials like MoS_2. In this mini-review, the research progress in ALD MoS_2 is firstly summarized. Then the influences of precursors, substrates, temperature, and post-annealing treatment on the quality of ALD-MoS_2 are presented. Moreover, the applications of the obtained MoS_2 as an electrochemical catalysator are also described. Besides the perspective on the research of ALD of MoS_2, the remaining challenges and promising potentials are also pointed out.**

Keywords: MoS_2, chemical vapor deposition (CVD), atomic layer deposition (ALD), two-dimensional (2D) materials

INTRODUCTION

Recently, as one of the dimensional (2-D) materials, MoS_2 has attracted wide attention owing to its excellent semiconducting and optical properties [1–5]. For layered MoS_2, the structure of hexagonal networks connected by covalent bonds of Mo and S atoms is very stable, and the weak interlayer-binding relies on the van der Waals force [6,7], which endows MoS_2 with the band-gap structure depending on the layer number strongly. When the bulk MoS_2 is exfoliated into monolayer, its band-gap will increase from ~1.2 eV (indirect) to ~1.8 eV (direct) [8,9]. Meanwhile, the current on/off ratio (1×10^8) and the carrier mobility (15 $cm^2\ V^{-1}\ s^{-1}$) at room temperature give MoS_2 huge possibilities in electronics and optoelectronics [6,10,11].

Continuous efforts are made for achieving monolayer or ultrathin MoS_2 films. Although mechanical exfoliation from bulk MoS_2 crystals is a common method to obtain monolayer MoS_2, the efficiency is too low to feed the demands of large-scale fabrications [12,13]. The chemical vapor deposition (CVD) has been a useful way to producing thin MoS_2 films by sulfurizing MoO_2 films between 850 and 950°C [14] or Mo films at 750°C [15], 900°C [16] and 1,050°C [17], directly depositing on Au [18], modified SiO_2 [19] or bare SiO_2 [20–22] between 530 and 800°C using Mo- and S-precursors, which indicates that the precursors, substrates and temperature influence the qualities of the obtained films. A flat substrate ensures the growth of a high quality MoS_2 film with a smooth surface and small lattice mismatch rather than nanostructures with large aspect ratios. However, the CVD method is unsuitable for mass fabrication owing to the poor reproducibility and reliability. As a kind of specially modified CVD, atomic layer deposition (ALD) is also used to grow thin films by the self-limiting chemical reaction. The chemical reaction in time sequence can be broken by dividing a complete reaction into two half-reactions in one ALD cycle. One half-reaction cannot stop until the active sites at the surface are depleted, then beginning the other half-reaction [23–27]. During the ALD, the chemical reaction on a new atomic layer is directly related to the previous layer, which makes every reaction only deposit one atomic layer. Due to the self-limiting reaction, not only the thickness of the films can be controlled at an atomic scale, but also the uniformity can be kept on a large-area substrate even with complex structures [28]. Moreover, ALD has a high reproducibility because the growth is insensitive to excessive precursors. Therefore, ALD has been an excellent method to fabricate 2-D MoS_2 films.

According to Fig. 1, where recent research progress in the preparation of MoS_2 by CVD [14–19,21–22] and ALD

[1] Industrial Center, Nanjing Institute of Technology, Nanjing 211167, China
[2] Jiangsu Key Laboratory for Design and Manufacture of Micro-Nano Biomedical Instruments, Southeast University, Nanjing 211189, China
* Corresponding author (email: liulei@seu.edu.cn)

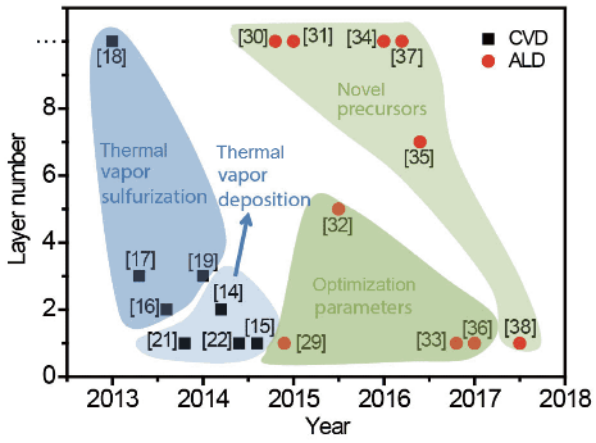

Figure 1 Research progress in the preparation of MoS_2 by CVD and ALD.

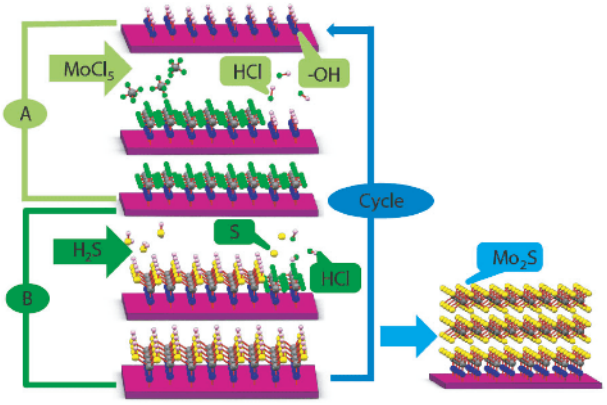

Figure 2 Schematic showing of the ALD of MoS_2.

[29–38] is shown, CVD contains two different means. One is the thermal vapor sulfurization where the MoS_2 film is obtained by sulfurizing the pre-deposited molybdenum film at high temperature. The other is thermal vapor deposition where Mo- and S-precursors enter the reactor at the same time to deposit the MoS_2 film. Like CVD, ALD also contains two different means. One is the optimization of process parameters while $MoCl_5$ and H_2S are used as the precursors. The other is to find the novel precursors. Although ALD of MoS_2 appears later, it will able to grow monolayer MoS_2 as same as the CVD.

Our group has been able to obtain monolayer MoS_2 directly by ALD, and the thickness of MoS_2 can be locally controlled layer by layer [36,39,40]. In this review, both the research progress in ALD of MoS_2 and the application prospect of the obtained MoS_2 as an electrochemical catalysator are shown. According to the discussion about the influences of the precursor, substrate, temperature, and post-annealing treatment on the quality of ALD-MoS_2, the challenges and potentials to obtain high-quality MoS_2 by ALD are also pointed out.

ALD OF MoS_2 FILMS

Tan *et al.* [29] firstly prepared MoS_2 by ALD on a sapphire substrate while $MoCl_5$ and H_2S were used as Mo- and S-precursors at 300°C. As shown in Fig. 2, one ALD cycle contains four steps: pulse and purge $MoCl_5$, pulse and purge H_2S. In the growth process, the corresponding chemical adsorption and reaction can be [39] (A) $Mo–SH^*+MoCl_5 \rightarrow Mo–S–MoCl_4^*+HCl$; (B) $MoCl^*+H_2S \rightarrow Mo–SH^*+HCl+S$, where * denotes the surface species.

$MoCl_5$ can be adsorbed to the substrate (A) or reacted with H_2S (B) by the self-limiting reaction. The MoS_2 films with a controllable thickness and uniform coverage can be fabricated by controlling the AB sequence. At the beginning, $MoCl_5$ is adsorbed to the bare substrate by the hydroxyl group, $|–OH^* + MoCl_5 \rightarrow |–O–MoCl_4^* + HCl$, where |– denotes the surface.

Therefore, the chemical functional group like hydroxyl on the substrate surface should be noticed in the initial growth, especially for mono- or few-layer MoS_2. In addition, there are two questions also need to be paid attention. On the one hand, the by-product contains HCl and S, which can corrode and damage the ALD reactor. On the other hand, because ALD is carried out at relatively low temperature, the as-grown MoS_2 always presents a low crystallinity and the post-annealing is usually necessary to achieve a high crystal quality. Accordingly, the precursor, substrate, temperature and post-annealing treatment have important influences on the quality of the MoS_2 film obtained by ALD. Therefore, these factors will be focused on in the next part.

Precursors and qualities of MoS_2 films obtained by ALD

Mo- and S-precursors may strongly affect the quality of MoS_2 obtained by ALD. However, it is a big challenge that finding or synthesizing suitable precursors for ALD of MoS_2. Furthermore, it is difficult to obtain a Mo-precursor that can rapidly react with H_2S, which is a frequently-used S-precursor in ALD of MoS_2. The reactivity and the volatility of the precursors ensure the self-limiting surface reaction. This depends on not only the fundamental chemical science but also the industrial engineering. The progress of the ALD technology is determined by the development of high quality precursors. Since $MoCl_5$ and H_2S as precursors opened the

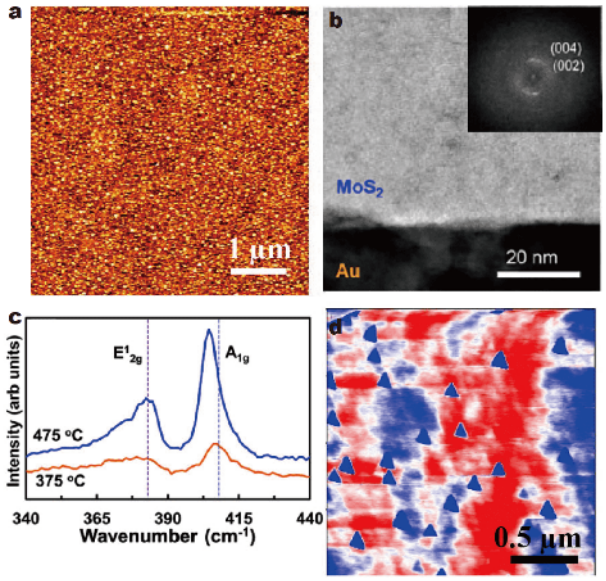

Figure 3 (a) AFM image for the MoS_2 film grown on sapphire at 300°C using $MoCl_5$ and H_2S. Reprinted with permission from Ref. [29], Copyright 2014, Royal Society of Chemistry. (b) TEM images for the MoS_2 film grown on Au at 250°C using $MoCl_5$ and H_2S. Reprinted with permission from Ref. [41], Copyright 2017, American Chemical Society. (c) Raman spectra comparing MoS_2 films obtained by ALD at 375 and 475°C. Reprinted with permission from Ref. [33], Copyright 2016, American Vacuum Society. (d) AFM image for the MoS_2 film grown on SiO_2 at 450°C using $MoCl_5$ and H_2S. Reprinted with permission from Ref. [36], Copyright 2017, IOP Publishing Ltd.

prelude of ALD of MoS_2 in 2014 [29], how to produce the high quality MoS_2 film by ALD has become a hot spot. On the one hand, the two precursors, $MoCl_5$ and H_2S are still used, and the film quality is improved by optimizing the process parameters [33,36,39–41]. On the other hand, the new precursors are tested [30,31,37,38,42–47].

For the first time, $MoCl_5$ and H_2S were used to grow the MoS_2 film on a sapphire substrate at 300°C. The atomic force microscopy (AFM) image of the as-grown MoS_2 film [29] is shown in Fig. 3a, where the grain with an obscure shape indicates the MoS_2 film is amorphous and the thickness per ALD cycle (GPC) is 0.21 nm/cycle. When the substrate is Au (Fig. 3b), the as-grown MoS_2 film is still amorphous [41] due to the low growth temperature. Subsequently, while the temperature rose to 475°C [33], the uniform MoS_2 film grown on a quartz substrate with the diameter of 150 mm can be obtained. According to Raman spectra (Fig. 3c), the crystallinity of the MoS_2 film grown at 475°C was obviously improved compared with that obtained at 375°C. Moreover, by the continuous optimization of process parameters, the MoS_2 film with triangle grains (Fig. 3d) was directly obtained at 450°C on a SiO_2 substrate without the post-annealing [36]. However, the grain size of ~100 nm is much smaller than that obtained by CVD. Continuous efforts have been made to find the new precursors with which the high quality MoS_2 film is directly obtained by ALD.

$Mo(NMe_2)_4$ with a high activity was used to react with H_2S for ALD of MoS_2 on the amorphous Al_2O_3 substrate at 150°C [38]. Owing to the high reactivity of $Mo(NMe_2)_4$, the reaction can be carried out at a very low temperature (80°C). The grown MoS_2 films can be directly patterned by the photolithography for the micro-nano devices on a large scale. However, the crystallinity of the obtained MoS_2 film is very poor due to the low temperature. $CH_3S_2CH_3$ was also used to react with $Mo(NMe_2)_4$ [45]. The obtained MoS_2 film with a poor crystallinity is also owing to the low growth temperature. While $Mo(CO)_6$ and $CH_3S_2CH_3$ were chosen as Mo- and S-precursors, the MoS_2 film can directly grow on a SiO_2/Si substrate at 100°C [30]. Thicknesses of the films against the exposure time of $Mo(CO)_6$ and $CH_3S_2CH_3$ were used to confirm the self-limiting reactions of the precursors. The grown MoS_2 film still has a low crystallinity owing to the low growth temperature. H_2S was also used to react with $Mo(CO)_6$ on a wafer-scale SiO_2/Si substrate at 165°C [35]. The grown MoS_2 film with a precise controllability and favorable uniformity is also amorphous. Moreover, the H_2S plasma with a higher reactivity was used to react with $Mo(CO)_6$ on SiO_2 at 175°C [37]. The MoS_2 film could also grow on a wafer-scale SiO_2 while $Mo(thd)_3$ and H_2S were used as precursors at 300°C [46]. Although, this is the highest growth temperature when the organometallic compounds are used as Mo-precursors, the films just have nano-crystalline structures.

Some precursors for ALD of MoS_2 that have been reported in literatures are listed in Table 1. The grain size and GPC of the grown MoS_2 film are variable with the precursor, substrate, and growth temperature. While $MoCl_5$ and H_2S are used as Mo- and S-precursors, the grain size increases from ~6.1 to ~120 nm as the growth temperature rises from 250 to 450°C, which indicates the higher temperature is propitious to ALD of MoS_2. Meanwhile, as novel Mo-precursors, metal-organic compounds such as $Mo(CO)_6$, $Mo(thd)_3$ and $Mo(NMe_2)_4$ exhibit higher reactivities than $MoCl_5$ at low temperature. The grown films have the favorable conformity and uniformity, but their crystallinity and GPC are low. As described above, metal-organic and metal-halide compounds are used as Mo-precursors for ALD of MoS_2, where the metal-organic presents a higher reactivity, lower crystallinity and GPC. Moreover,

Table 1 Various Mo- and S- precursors for ALD of MoS_2

Mo-precursor	S-precursor	Temp. (°C)	Substrate	GPC (nm/cycle)	Grain size	Ref.
$MoCl_5$	H_2S	300	Sapphire	0.21	Amorphous	[29]
$MoCl_5$	H_2S	250	Au	/	6.1 nm	[41]
$MoCl_5$	H_2S	375	SiO_2	0.025	Amorphous	[33]
$MoCl_5$	H_2S	430–470	Si, SiO_2	0.38	35–120 nm	[39,40]
$MoCl_5$	H_2S	450	SiO_2	0.65	100 nm	[36]
$Mo(CO)_6$	$CH_3S_2CH_3$	100–120	SiO_2	0.11	Amorphous	[30]
$Mo(CO)_6$	H_2S	155–175	Co, SiO_2	0.074	Amorphous	[43,35]
$Mo(CO)_6$	H_2S plasma	175–200	SiO_2	0.05	20 nm	[37]
$Mo(NMe_2)_4$	H_2S	60–120	Al_2O_3	/	Amorphous	[38]
$Mo(CO)_6$	H_2S plasma	200	Si	/	5–20 nm	[42]
$Mo(thd)_3$	H_2S	300	Si, etc.	0.025	10–30 nm	[46]
$Mo(NMe_2)_4$	$CH_3S_2CH_3$	50	SiO_2	/	Amorphous	[45]
MoF_6	H_2S	200	Si	0.06	Amorphous	[47]

although the grain size can be increased by elevating the growth temperature, it is still much smaller than that obtained by CVD. Therefore, the precursors that can be directly and safely used to fabricate the MoS_2 film with high quality are still in need.

ALD temperature windows of MoS_2

ALD is carried out within a temperature range, the ALD window related to the precursors [48]. As shown in Fig. 4a, the ALD window of $MoCl_5$ and H_2S is kept in 440–470°C [39]. If the temperature is lower than 440°C, the surface reactions will be incomplete. The chemical reactivity and occupation of $MoCl_5$ and H_2S can be improved by elevating the temperature. However, if the temperature is higher than 470°C, the re-evaporation of the grown MoS_2 film leads to the decrease of GPC. While $Mo(CO)_6$ is used to replace $MoCl_5$ as Mo-precursor [35], the ALD window shown in Fig. 4b is in the range of 155–175°C. The surface reactions will also be incomplete at the temperature lower than the floor of the window. However, above the window, unlike $MoCl_5$, the disordered stacks from the thermal decomposition of $Mo(CO)_6$ bring an increase of GPC. While the other metal-organic $Mo(NMe_2)_4$ and $Mo(thd)_3$ are used as Mo-precursors, ALD windows are 60–120 and 275–325°C, respectively [38,46].

Compared with CVD, the lower temperature of ALD leads to the MoS_2 film with a lower crystallinity. Moreover, while the metal-halide is used as the Mo-precursor, the higher ALD window brings the higher crystallinity of MoS_2. As described above, the ALD window depends on the activity of the precursor, and

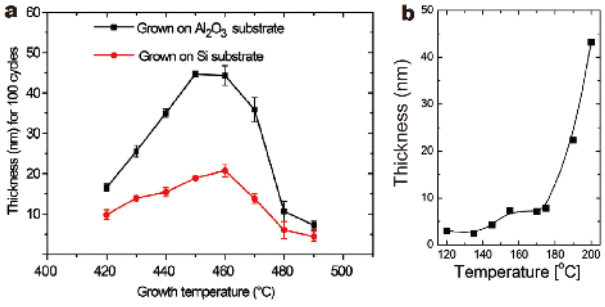

Figure 4 ALD temperature windows using different precursors. (a) $MoCl_5$ and H_2S. Reprinted with permission from Ref. [39], Copyright 2017, Elsevier. (b) $Mo(CO)_6$ and H_2S. Reprinted with permission from Ref. [35], Copyright 2014, Royal Society of Chemistry.

the MoS_2 film with a high crystallinity needs to grow at a high temperature in the window.

ALD substrates of MoS_2

As mentioned above, an ALD cycle contains two individual self-limiting surface reactions. Within the ALD window, it is necessary that a full coverage of monolayer can be realized by the precursor pulse, and the surface reactions will stop by themselves owing to the exhaustion of surface active sites, which endows ALD with a stable GPC and makes it insensitive to any further increase of the pulse length. By this stable GPC coming from the self-limiting reactions, the uniform and ultrathin MoS_2 films can grow on the substrates even with complex structures, such as wires, powders, tubes, and holes/pores [25–27], which are the uniqueness of ALD. According to the crystallinity and orientation of the MoS_2 films, not only the precursors but also the

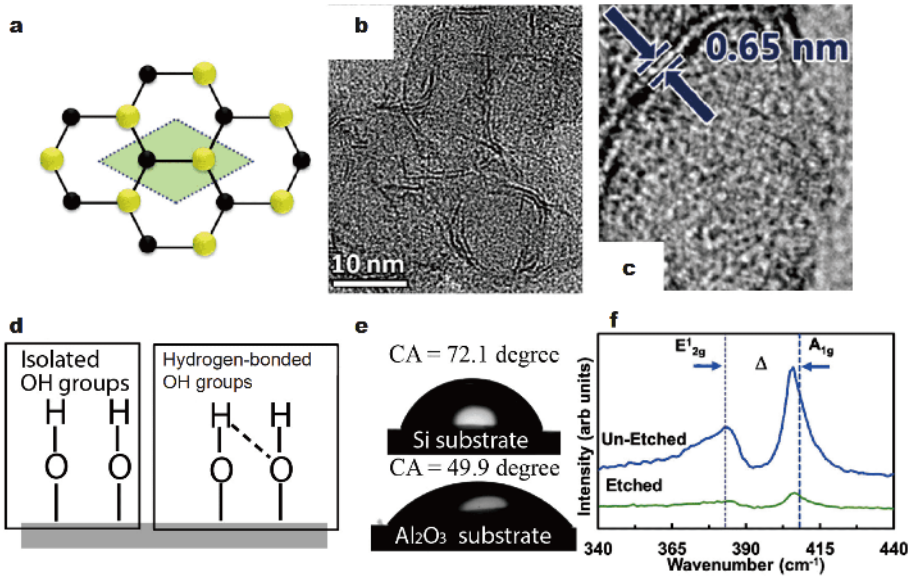

Figure 5 (a) A top view of MoS_2. Reprinted with permission from Ref. [49], Copyright 2013, American Vacuum Society. (b) TEM image of MoS_2 by ALD on silica nano-bead. (c) d_{0001} spacing. Reprinted with permission from Ref. [45], Copyright 2017, Royal Society of Chemistry. (d) Hydroxyl groups on the surface of the substrate. (e) Water contact angles of Si and Al_2O_3 substrates. Reprinted with permission from Ref. [39], Copyright 2017, Elsevier. (f) Raman spectra for ALD MoS_2 films on etched and unetched substrate. Reprinted with permission from Ref. [33], Copyright 2016, American Vacuum Society.

substrates play an important role in ALD of MoS_2.

On a sapphire substrate, the triangular grain with the size of ~2 μm can be obtained (by post-annealing) [29]. This may be attributed to the hexagonal crystal structure of the sapphire. The atomically smooth (RMS<0.1 nm) C-planes matches the (0001) planes of 2-H MoS_2 (Fig. 5a). This is propitious to the nucleation and growth of the large-size monocrystal MoS_2 [49,50]. When the MoS_2 film is coated on a silica nano-bead surface [45], the (0001) planes of MoS_2 perpendicular to the substrate can be observed (Fig. 5b, c). This structure can increase the number of active edge sites of the MoS_2 films. In addition, the species and density of hydroxyl groups on the substrates are also very important to ALD of MoS_2, especially for mono- or few-layer MoS_2. In the initial stage of ALD, the MoS_2 films are chemically adsorbed on the substrates through the hydroxyl groups. There are two different hydroxyl groups on the surface of substrates (Fig. 5d), hydrogen-bonded hydroxyl and isolated hydroxyl [51–53]. Above 200°C, dehydroxylation will remove the hydrogen-bonded hydroxyl groups firstly. However, the isolated hydroxyl groups keep stable under 400°C [52]. Therefore, to obtain high quality MoS_2 films, the interference of hydrogen-bonded hydroxyl should be excluded. A preheating process of the substrate at about 200°C before the growth is necessary. The acid washing and the oxygen plasma treatment can increase the density of hydroxyl groups on the surface of substrates. Moreover, the density can also be increased by covering the hydroxyl-rich seed layer on the substrates. The amorphous Al_2O_3 with abundant hydroxyl groups (Fig. 5e) is more suitable for ALD of MoS_2 than the Si substrate [39]. The microcosmic surface structure of the substrates will also affect the crystallinity of the MoS_2 films. According to the Raman spectra (Fig. 5f), the obtained MoS_2 films on the etched SiO_2 substrates have a higher crystallinity than those on the unetched substrates [33]. To obtain the high-quality MoS_2 films, the crystal structure, surface functional groups and microcosmic structure of the substrate need to be considered.

POST-ANNEALING OF MoS_2 OBTAINED BY ALD

Due to the low ALD window of MoS_2, the as-deposited MoS_2 films are commonly amorphous and/or nanocrystalline. To obtain the high crystallinity MoS_2 film, post-annealing at the elevated temperature is usually necessary. In the post-annealing process, parameters such as the temperature, temperature-ramping speed, duration, and environment (Ar_2 and/or S_2 atmosphere) should be considered. For the conventional semiconductor thin films [54,55], some changes usually in the heat treatments such as defects annihilation, stress build-up and release, morphological changes, and dopant activation may also

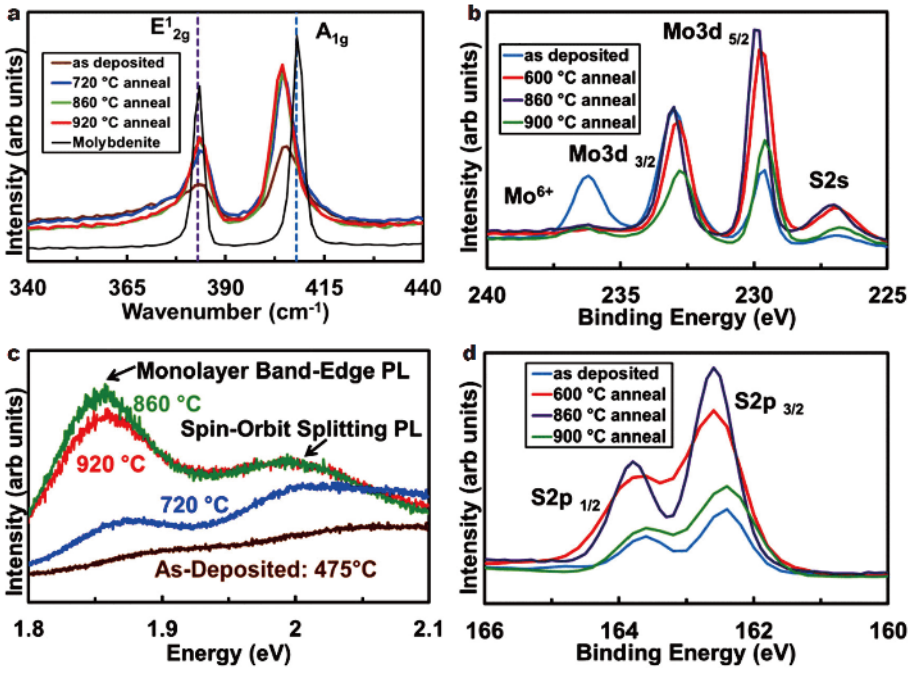

Figure 6 (a) Raman spectra of the as-deposited and sulfur-annealed MoS_2 films. (b) Corresponding photoluminescence spectra. XPS spectra of Mo (c) and S (d). Reprinted with permission from Ref. [33], Copyright 2016, American Vacuum Society.

appear in the crystallization induced by post-annealing to the as-grown MoS_2 films. Although the nano-crystalline MoS_2 films can directly grow by ALD at 475°C using $MoCl_5$ and H_2S as precursors, the crystallinity of the films can be improved by post-annealing in sulfur atmosphere [33]. Raman spectra of MoS_2 films before and after annealing are shown in Fig. 6a, where the full width half maximum (FWHM) of E^1_{2g} and A_{1g} peaks is used to indicate the crystallinity. After post-annealing in sulfur atmosphere above 700°C, the two peaks become strong and narrow, which indicates the high crystallinity of the as-grown MoS_2 films. This can also be confirmed by the change of photoluminescence (PL) peaks before and after annealing (Fig. 6b). The X-ray photoelectron spectroscopy (XPS) of the as-grown and sulfur annealed MoS_2 films are shown in Fig. 6c, d. The stoichiometric ratios of the films before and after post-annealing are determined by the intensity ratios of S $2p_{3/2}$ and Mo $3d_{5/2}$ peaks. The increase of the S/Mo ratio from 1.4 to 2.0 after annealing above 600°C suggests the improved substoichiometric sulfur ratio by high-temperature annealing in sulfur atmosphere.

The amorphous MoS_2 (Fig. 7a) can be transformed into triangular MoS_2 grains (Fig. 7b) with a size of ~2 μm on the sapphire after annealing at 800°C in sulfur ambient [29]. This is the largest monocrystalline MoS_2 grown by

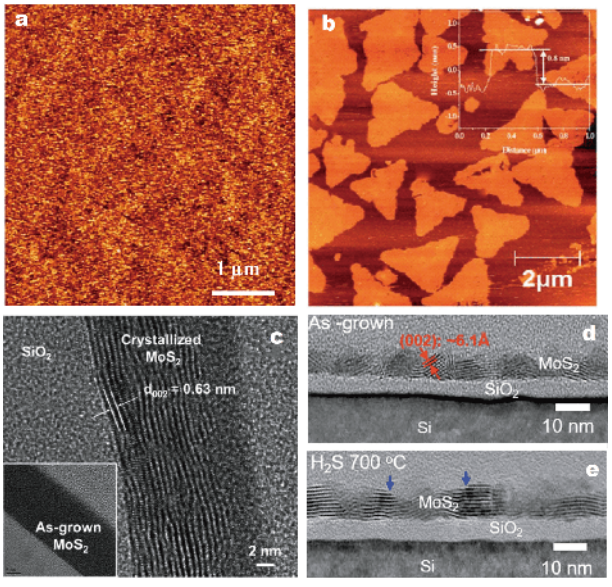

Figure 7 AFM images for as-grown (a) and annealed (b) MoS_2 films on sapphire substrates. Reprinted with permission from Ref. [29], Copyright 2014, Royal Society of Chemistry. (c) Cross-sectional TEM images of the MoS_2 film annealed at 900°C. Reprinted with permission from Ref. [30], Copyright 2014, Royal Society of Chemistry. Cross-sectional TEM images of as-grown (d) and sulfurized (e) MoS_2 on p-Si wafers at 700°C. Reprinted with permission from Ref. [42], Copyright 2017, Royal Society of Chemistry.

Table 2 Post-annealing processes of as-grown MoS_2 films

As-grown				Post-annealing				
Mo-precursor	S-precursor	S/Mo	Grain size	Temp. (°C)	S/Mo	Grain size	Atmosphere	Ref.
$MoCl_5$	H_2S	1.97	Amorphous	800	2.03	20 μm	S	[29]
$Mo(CO)_6$	$CH_3S_2CH_3$	1.21	Amorphous	900	2.01	Nano-crystalline	Ar	[30]
$MoCl_5$	H_2S	1.4	Amorphous	860–920	2	Nano-crystalline	H_2S, S	[33]
$Mo(CO)_6$	H_2S	1.5	Amorphous	900	2	Nano-crystalline	H_2S, Ar	[35]
$Mo(NMe_2)_4$	H_2S	/	Amorphous	1,000	/	200 nm	S	[38]
$Mo(CO)_6$	H_2S plasma	1	6–10 nm	600	2	14 nm	H_2S	[42]

ALD so far, which reveals the great potential of ALD in producing crystalline MoS_2. Amorphous MoS_2 has been obtained on the amorphous Al_2O_3 [38]. After annealing for 5 h at 1,000°C in sulfur ambient, the crystalline MoS_2 film consisting of crystallites (~20 nm) can be observed. The as-grown amorphous MoS_2 also can be parallel to the SiO_2 substrate (Fig. 7c) after annealing for 5 min at 900°C in Ar ambient [30]. Cross-sectional TEM images of MoS_2 grown at 200°C and annealed at 700°C on p-Si wafers [42] are shown in Fig. 7d, e. The grain sizes of the as-grown MoS_2 are in the range of about 6–10 nm and the (002) plane spacing is about 6.1 Å. When the post-annealing is carried out at 700°C in sulfur ambient, MoS_2 grains grow to about 14 nm and the (002) plane of MoS_2 will be in parallel to the Si substrate. These indicate the crystallinity is improved after post-annealing. The MoS_2 obtained by post-annealing is the 2H phase. Thermodynamically, the 2H phase is more stable than 1T and 1T' phases. They can be transformed into the 2H phase under heating. Post-annealing of the MoS_2 films are shown in Table 2. The temperature above 600°C and the atmosphere such as S, H_2S, and Ar are generally used for annealing the as-grown MoS_2. The crystallinity and substoichiometric sulfur of the as-grown MoS_2 films can be improved by the high-temperature annealing. Because the ALD temperature of MoS_2 is relatively low, post-annealing is required to obtain the MoS_2 films with a high crystallinity. Not only the crystallinity but also the substoichiometric sulfur of the MoS_2 films can be improved by post-annealing.

APPLICATIONS OF MoS_2 OBTAINED BY ALD

Pt is considered to be the most efficient catalyst for the electrochemical hydrogen evolution reaction (HER). However, Pt is insufficient and expensive. In fact, the HER activity is generally determined by the Gibbs free energy of hydrogen adsorption (ΔG_{H^*}) [56,57]. Although MoS_2 as a HER catalyst has become a hot spot of research due to the small ΔG_{H^*} on its edge sites [58], how to conveniently and economically increase the edge sites is still a problem for improving the HER activity [59–62]. Recently, amorphous or nanocrystal MoS_2 obtained by ALD exhibits a high HER activity because they can enlarge the area of exposed edge sites [31,34,41,42].

HER polarization curves of a bare Au and two MoS_2 films with different thickness obtained by ALD are shown in Fig. 8a. When the current density reaches 100 μA cm^{-2}, the overpotential is designated as the onset potential. The onset potentials (165 and 181 mV) of thick and thin MoS_2 films are much smaller than that of bare Au (222 mV), which indicates the MoS_2 films have a better activity than the bare Au and the activity can be improved by increasing the thickness. HER polarization curves of the bare carbon fiber paper (CFP) and MoS_2 films obtained by different ALD cycles are shown in Fig. 8b. For the MoS_2/Au catalyst, the overpotential of 254 mV is needed at the current density of 5 mA cm^{-2}. However, at the same overpotential, the double current density can be obtained in the MoS_2/CFP catalyst, which may be owing to the large active surface area. Tafel slope b and exchange current density j_0 obtained from Fig. 8a and b are listed in Table 3. Although the j_0 of bare Au is about 1 order of magnitude bigger than that of MoS_2 obtained by ALD, much smaller Tafel slope (47−50 mV dec^{-1}) of MoS_2 than that (88 mV dec^{-1}) of Au indicates MoS_2 has a better HER activity than Au [62]. HER mechanism of ALD-MoS_2 catalysts is the same because the Tafel slopes of ALD-MoS_2 catalysts are in a small range (47–57 mV dec^{-1}), and the main pathway for the HER may be the VH (Volmer-Heyrovsky) [63].

Moreover, a type II heterojunction can be formed by coating MoS_2 on Si [64–66]. In the MoS_2/Si heterostructure, photoexcited electrons in Si will also participate in the HER by transporting to the Si/MoS_2 and MoS_2/H_2O interfaces. Nanocrystal MoS_2 films grew on p-Si by ALD

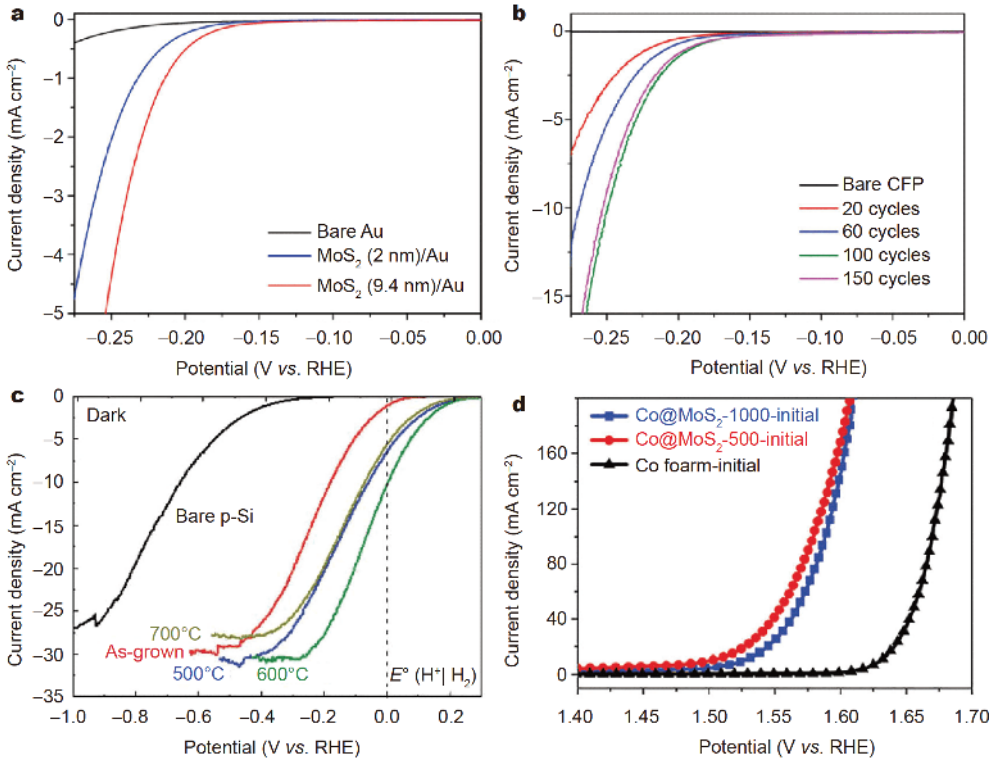

Figure 8 (a) HER polarization curves of bare Au and MoS_2/Au. Reprinted with permission from Ref. [31], Copyright 2015, American Chemical Society. (b) HER polarization curves of bare CFP and MoS_2/CFP. Reprinted with permission from Ref. [34], Copyright 2016, Royal Society of Chemistry. (c) PEC HER polarization curves of bare p-Si, as-grown and sulfurized MoS_2/p-Si. Reprinted with permission from Ref. [42], Copyright 2017, Royal Society of Chemistry. (d) OER polarization curves of bare Co foam and Co@MoS_2-500 grown by various cycles. Reprinted with permission from Ref. [43], Copyright 2017, Royal Society of Chemistry.

Table 3 Electrocatalytic activity of MoS_2 obtained by ALD

Sample	Tafel slope (mV dec^{-1})	J_0 (μA cm^{-2})	TOF at 0.2 V *vs.* RHE (H_2 s^{-1})	Ref.
Bare Au	88	0.293	/	[31]
MoS_2 (2.0 nm)	50	0.024	/	
MoS_2 (9.4 nm)	47	0.027	1.45	
Bare CFP	/	/	/	[34]
MoS_2 (20 cycles)	56.6	0.025	0.2–0.5	
MoS_2 (60 cycles)	56.5	0.039	0.3–0.8	
MoS_2 (100 cycles)	55.8	0.039	0.4–0.9	
MoS_2 (150 cycles)	55.6	0.027	0.3–0.7	

using $Mo(CO)_6$ and H_2S at 200°C. Bare p-Si, as-grown MoS_2/p-Si, and post-annealing MoS_2/p-Si were used for the photoelectrochemical (PEC) H_2 [42]. Their PEC polarization curves are shown in Fig. 8c, where the overpotential of MoS_2/p-Si is much smaller than that of bare p-Si at the same current density, indicating ALD-MoS_2 can obviously improve the PEC activity. ALD-MoS_2 was also used as a catalyst for the O_2 evolution reaction (OER) [43,67,68]. The OER polarization curves of bare Co, Co@MoS_2-500 and Co@MoS_2-1000 are shown in Fig. 8d, where the overpotential of Co@MoS_2 is much smaller than that of bare Co at the same current density, indicating the ALD-MoS_2 has a better catalytic activity for OER. Moreover, the similar polarization curves of Co@MoS_2-500 and Co@MoS_2-1000 indicate the catalytic activity is insensitive to the thickness of MoS_2.

As described above, as an electrochemical catalyst, ALD-MoS_2 has the excellent catalytic activity both for HER and OER. The catalytic activity is insensitive to the number of cycles till it forms a continuous MoS_2 film. However, the thickness of MoS_2 has influence on the properties of Si/MoS_2 heterostructures such as the optical absorption, charge separation, and recombination, and thus affects the PEC activity. ALD-MoS_2 with the amorphous structure has higher activity than that with the nanocrystal structure owing to the abundant active sites. Moreover, post-annealing can further improve the activity of MoS_2, because annealing can make the grain perpendicular to the substrate and expose more active edges.

Therefore, there are two aspects needing to be paid attention to for improving the catalytic activity of ALD-MoS_2. The one is to make the MoS_2 grain as small as possible and perpendicular to the substrate, thus exposing as many active sites as possible, which can be achieved by controlling the processes of the growth and post-annealing. In order to obtain the MoS_2 grain with a small size, ALD should be carried out by using the metal-organic compound with a high reactivity as the Mo-precursor, and the substrate should avoid the plasma clean to keep the low surface energy. The MoS_2 grain perpendicular to the substrate can be obtained by controlling post-annealing parameters such as the temperature, rates of heating and cooling. The other is to improve the conductivity of MoS_2 through the doping of the conductive metal like Cu and Ag. However, it is a challenge that keeping the small ΔG_{H^*} of MoS_2 edge unchangeable when the doping is introduced.

CONCLUSION AND OUTLOOK

In the ALD process, precursors, substrates, temperature and post-annealing treatments have influences on the quality of the MoS_2 films. To directly and safely obtain high-quality MoS_2 films by ALD, searching for novel precursors and optimizing process parameters are necessary. Metal-organic compound and metal-halide are used as Mo-precursors to deposit the MoS_2 films. Metal-organic compound has a high reactivity while the obtained MoS_2 films have a low crystallinity and GPC. Crystal structures, surface functional groups and micro-structures of the substrates are also very important to ALD of MoS_2. Hexagonal crystal substrates, acid pickling or plasma treating to increase the hydroxyl density of the substrate surface, annealing the substrate at ~200°C to vanish the hydrogen-bonded hydroxyl groups may be useful for obtaining high crystalline MoS_2 films by ALD. Although the growth temperature is elevated to enlarge the size of the MoS_2 grain obtained by ALD, the grain is still much smaller than that obtained by CVD. Therefore, in order to improve the crystalline quality, the post-annealing is necessary.

Although the crystallinity of MoS_2 obtained by ALD is lower than that obtained by CVD, the ALD-MoS_2 film has shown excellent electrochemical properties as a catalysator in HER, OER, and PEC, which benefits from the abundant activity sites. The remaining challenge is how to improve the conductivity of ALD-MoS_2 and keep the small ΔG_{H^*} unchangeable at the same time.

Adhesion and friction between contact surfaces seriously hinder the reliability and performance of the micro-electro-mechanical system (MEMS). In order to solve the problems, lubricant and protective films are usually coated on the surface of MEMS. Comparing with traditional technologies such as physical or chemical vapor deposition (PVD or CVD), ALD can easily deal with the challenge that how to conformally coat the film on the three-dimensional structure of MEMS. Therefore, as an excellent lubricating material, the MoS_2 film obtained by ALD may provide the low friction surface required in MEMS.

Received 11 December 2018; accepted 12 February 2019; published online 4 March 2019

1 Radisavljevic B, Radenovic A, Brivio J, *et al.* Single-layer MoS_2 transistors. Nat Nanotechnol, 2011, 6: 147–150
2 Ghatak S, Pal AN, Ghosh A. Nature of electronic states in atomically thin MoS_2 field-effect transistors. ACS Nano, 2011, 5: 7707–7712
3 Baugher BWH, Churchill HOH, Yang Y, *et al.* Intrinsic electronic transport properties of high-quality monolayer and bilayer MoS_2. Nano Lett, 2013, 13: 4212–4216
4 Wang F, Stepanov P, Gray M, *et al.* Annealing and transport studies of suspended molybdenum disulfide devices. Nanotechnology, 2015, 26: 105709
5 Wang F, Stepanov P, Gray M, *et al.* Ionic liquid gating of suspended MoS_2 field effect transistor devices. Nano Lett, 2015, 15: 5284–5288
6 Wang QH, Kalantar-Zadeh K, Kis A, *et al.* Electronics and optoelectronics of two-dimensional transition metal dichalcogenides. Nat Nanotechnol, 2012, 7: 699–712
7 Bertrand PA. Surface-phonon dispersion of MoS_2. Phys Rev B, 1991, 44: 5745–5749
8 Kam KK, Parkinson BA. Detailed photocurrent spectroscopy of the semiconducting group VIB transition metal dichalcogenides. J Phys Chem, 1982, 86: 463–467
9 Mak KF, Lee C, Hone J, *et al.* Atomically thin MoS_2: a new direct-gap semiconductor. Phys Rev Lett, 2010, 105: 136805
10 Wu S, Ross JS, Liu GB, *et al.* Electrical tuning of valley magnetic moment through symmetry control in bilayer MoS_2. Nat Phys, 2013, 9: 149–153

11 Mak KF, He K, Shan J, *et al.* Control of valley polarization in monolayer MoS_2 by optical helicity. Nat Nanotechnol, 2012, 7: 494–498
12 Gurarslan A, Yu Y, Su L, *et al.* Surface-energy-assisted perfect transfer of centimeter-scale monolayer and few-layer MoS_2 films onto arbitrary substrates. ACS Nano, 2014, 8: 11522–11528
13 Eda G, Yamaguchi H, Voiry D, *et al.* Photoluminescence from chemically exfoliated MoS_2. Nano Lett, 2011, 11: 5111–5116
14 Wang X, Feng H, Wu Y, *et al.* Controlled synthesis of highly crystalline MoS_2 flakes by chemical vapor deposition. J Am Chem Soc, 2013, 135: 5304–5307
15 Zhan Y, Liu Z, Najmaei S, *et al.* Large-area vapor-phase growth and characterization of MoS_2 atomic layers on a SiO_2 substrate. Small, 2012, 8: 966–971
16 Laskar MR, Ma L, Kannappan S, *et al.* Large area single crystal (0001) oriented MoS_2. Appl Phys Lett, 2013, 102: 252108
17 Tarasov A, Campbell PM, Tsai MY, *et al.* Highly uniform trilayer molybdenum disulfide for wafer-scale device fabrication. Adv Funct Mater, 2014, 24: 6389–6400
18 Shi J, Ma D, Han GF, *et al.* Controllable growth and transfer of monolayer MoS_2 on Au foils and its potential application in hydrogen evolution reaction. ACS Nano, 2014, 8: 10196–10204
19 Lee YH, Zhang XQ, Zhang W, *et al.* Synthesis of large-area MoS_2 atomic layers with chemical vapor deposition. Adv Mater, 2012, 24: 2320–2325
20 Yang S, Kang J, Yue Q, *et al.* Vapor phase growth and imaging stacking order of bilayer molybdenum disulfide. J Phys Chem C, 2014, 118: 9203–9208
21 van der Zande AM, Huang PY, Chenet DA, *et al.* Grains and grain boundaries in highly crystalline monolayer molybdenum disulphide. Nat Mater, 2013, 12: 554–561
22 Zhang J, Yu H, Chen W, *et al.* Scalable growth of high-quality polycrystalline MoS_2 monolayers on SiO_2 with tunable grain sizes. ACS Nano, 2014, 8: 6024–6030
23 Kong L, Wang Q, Xiong S, *et al.* Turning low-cost filter papers to highly efficient membranes for oil/water separation by atomic-layer-deposition-enabled hydrophobization. Ind Eng Chem Res, 2014, 53: 16516–16522
24 Zhou Y, King DM, Li J, *et al.* Synthesis of photoactive magnetic nanoparticles with atomic layer deposition. Ind Eng Chem Res, 2010, 49: 6964–6971
25 Miikkulainen V, Leskelä M, Ritala M, *et al.* Crystallinity of inorganic films grown by atomic layer deposition: overview and general trends. J Appl Phys, 2013, 113: 021301
26 Leskelä M, Ritala M, Nilsen O. Novel materials by atomic layer deposition and molecular layer deposition. MRS Bull, 2011, 36: 877–884
27 George SM. Atomic layer deposition: an overview. Chem Rev, 2010, 110: 111–131
28 Leskelä M, Ritala M. Atomic layer deposition chemistry: recent developments and future challenges. Angew Chem Int Ed, 2003, 42: 5548–5554
29 Tan LK, Liu B, Teng JH, *et al.* Atomic layer deposition of a MoS_2 film. Nanoscale, 2014, 6: 10584–10588
30 Jin Z, Shin S, Kwon DH, *et al.* Novel chemical route for atomic layer deposition of MoS_2 thin film on SiO_2/Si substrate. Nanoscale, 2014, 6: 14453–14458
31 Shin S, Jin Z, Kwon DH, *et al.* High turnover frequency of hydrogen evolution reaction on amorphous MoS_2 thin film directly grown by atomic layer deposition. Langmuir, 2015, 31: 1196–1202
32 Browning R, Padigi P, Solanki R, *et al.* Atomic layer deposition of MoS_2 thin films. Mater Res Express, 2015, 2: 035006
33 Valdivia A, Tweet DJ, Conley Jr. JF. Atomic layer deposition of two dimensional MoS_2 on 150 mm substrates. J Vacuum Sci Tech A-Vacuum Surfs Films, 2016, 34: 021515
34 Kwon DH, Jin Z, Shin S, *et al.* A comprehensive study on atomic layer deposition of molybdenum sulfide for electrochemical hydrogen evolution. Nanoscale, 2016, 8: 7180–7188
35 Pyeon JJ, Kim SH, Jeong DS, *et al.* Wafer-scale growth of MoS_2 thin films by atomic layer deposition. Nanoscale, 2016, 8: 10792–10798
36 Liu L, Huang Y, Sha J, *et al.* Layer-controlled precise fabrication of ultrathin MoS_2 films by atomic layer deposition. Nanotechnology, 2017, 28: 195605
37 Jang Y, Yeo S, Lee HBR, *et al.* Wafer-scale, conformal and direct growth of MoS_2 thin films by atomic layer deposition. Appl Surf Sci, 2016, 365: 160–165
38 Jurca T, Moody MJ, Henning A, *et al.* Low-temperature atomic layer deposition of MoS_2 films. Angew Chem Int Ed, 2017, 56: 4991–4995
39 Huang Y, Liu L, Zhao W, *et al.* Preparation and characterization of molybdenum disulfide films obtained by one-step atomic layer deposition method. Thin Solid Films, 2017, 624: 101–105
40 Huang Y, Liu L, Sha J, *et al.* Size-dependent piezoelectricity of molybdenum disulfide (MoS_2) films obtained by atomic layer deposition (ALD). Appl Phys Lett, 2017, 111: 063902
41 Ho TA, Bae C, Lee S, *et al.* Edge-on MoS_2 thin films by atomic layer deposition for understanding the interplay between the active area and hydrogen evolution reaction. Chem Mater, 2017, 29: 7604–7614
42 Oh S, Kim JB, Song JT, *et al.* Atomic layer deposited molybdenum disulfide on Si photocathodes for highly efficient photoelectrochemical water reduction reaction. J Mater Chem A, 2017, 5: 3304–3310
43 Xiong D, Zhang Q, Li W, *et al.* Atomic-layer-deposited ultrafine MoS_2 nanocrystals on cobalt foam for efficient and stable electrochemical oxygen evolution. Nanoscale, 2017, 9: 2711–2717
44 Zhang T, Wang Y, Xu J, *et al.* High performance few-layer MoS_2 transistor arrays with wafer level homogeneity integrated by atomic layer deposition. 2D Mater, 2018, 5: 015028
45 Cadot S, Renault O, Frégnaux M, *et al.* A novel 2-step ALD route to ultra-thin MoS_2 films on SiO_2 through a surface organometallic intermediate. Nanoscale, 2017, 9: 538–546
46 Mattinen M, Hatanpää T, Sarnet T, *et al.* Atomic layer deposition of crystalline MoS_2 thin films: new molybdenum precursor for low-temperature film growth. Adv Mater Interfaces, 2017, 4: 1700123
47 Mane AU, Letourneau S, Mandia DJ, *et al.* Atomic layer deposition of molybdenum disulfide films using MoF_6 and H_2S. J Vacuum Sci Tech A-Vacuum Surfs Films, 2018, 36: 01A125
48 Liu H. Recent progress in atomic layer deposition of multifunctional oxides and two-dimensional transition metal dichalcogenides. J Mol Eng Mater, 2016, 04: 1640010
49 Xu M, Liang T, Shi M, *et al.* Graphene-like two-dimensional materials. Chem Rev, 2013, 113: 3766–3798
50 Huang H, Li X, Xu X. An experimental research on the force and energy during the sapphire sawing using reciprocating electroplated diamond wire saw. J Manuf Sci Eng, 2017, 139: 121011
51 Mathieu MV, Primet M, Pichat P. Infrared study of the surface of titanium dioxides. II. Acidic and basic properties. J Phys Chem, 1971, 75: 1221–1226

52 Primet M, Pichat P, Mathieu MV. Infrared study of the surface of titanium dioxides. I. Hydroxyl groups. J Phys Chem, 1971, 75: 1216–1220
53 Bezrodna T, Puchkovska G, Shymanovska V, *et al.* IR-analysis of H-bonded H_2O on the pure TiO_2 surface. J Mol Struct, 2004, 700: 175–181
54 Liu H, Chi D. Magnetron-sputter deposition of Fe_3S_4 thin films and their conversion into pyrite (FeS_2) by thermal sulfurization for photovoltaic applications. J Vacuum Sci Tech A-Vacuum Surfs Films, 2012, 30: 04D102
55 Li ZQ, Chen H, Liu HF, *et al.* Influence of Si doping on optical characteristics of cubic GaN grown on (001) GaAs substrates. Appl Phys Lett, 2000, 76: 3765–3767
56 Conway BE, Bockris JOM. Electrolytic hydrogen evolution kinetics and its relation to the electronic and adsorptive properties of the metal. J Chem Phys, 1957, 26: 532–541
57 Nørskov JK, Bligaard T, Rossmeisl J, *et al.* Towards the computational design of solid catalysts. Nat Chem, 2009, 1: 37–46
58 Hinnemann B, Moses PG, Bonde J, *et al.* Biomimetic hydrogen evolution: MoS_2 nanoparticles as catalyst for hydrogen evolution. J Am Chem Soc, 2005, 127: 5308–5309
59 Jaramillo TF, Jørgensen KP, Bonde J, *et al.* Identification of active edge sites for electrochemical H_2 evolution from MoS_2 nanocatalysts. Science, 2007, 317: 100–102
60 Karunadasa HI, Montalvo E, Sun Y, *et al.* A molecular MoS_2 edge site mimic for catalytic hydrogen generation. Science, 2012, 335: 698–702
61 Kibsgaard J, Jaramillo TF, Besenbacher F. Building an appropriate active-site motif into a hydrogen-evolution catalyst with thiomolybdate $[Mo_3S_{13}]^{2-}$ clusters. Nat Chem, 2014, 6: 248–253
62 Conway BE, Tilak BV. Interfacial processes involving electrocatalytic evolution and oxidation of H_2, and the role of chemisorbed H. Electrochim Acta, 2002, 47: 3571–3594
63 Li Y, Wang H, Xie L, *et al.* MoS_2 nanoparticles grown on graphene: an advanced catalyst for the hydrogen evolution reaction. J Am Chem Soc, 2011, 133: 7296–7299
64 Tsai ML, Su SH, Chang JK, *et al.* Monolayer MoS_2 heterojunction solar cells. ACS Nano, 2014, 8: 8317–8322
65 Merki D, Fierro S, Vrubel H, *et al.* Amorphous molybdenum sulfide films as catalysts for electrochemical hydrogen production in water. Chem Sci, 2011, 2: 1262–1267
66 Kwon KC, Choi S, Hong K, *et al.* Wafer-scale transferable molybdenum disulfide thin-film catalysts for photoelectrochemical hydrogen production. Energy Environ Sci, 2016, 9: 2240–2248
67 McCrory CCL, Jung S, Ferrer IM, *et al.* Benchmarking hydrogen evolving reaction and oxygen evolving reaction electrocatalysts for solar water splitting devices. J Am Chem Soc, 2015, 137: 4347–4357
68 Wang J, Cui W, Liu Q, *et al.* Recent progress in cobalt-based heterogeneous catalysts for electrochemical water splitting. Adv Mater, 2016, 28: 215–230

Acknowledgements This work is financially supported by the National Natural Science Foundation of China (51822501), the Natural Science Funds for Distinguished Young Scholar of Jiangsu Province (BK20170023), the Fundamental Research Funds for the Central Universities (3202006301 and 3202006403), Qing Lan Project of Jiangsu Province, the International Foundation for Science, Stockholm, Sweden, the Organization for the Prohibition of Chemical Weapons, the Hague, Netherlands, through a grant to Lei Liu (F/4736-2), the grants from Top 6 High-Level Talents Program of Jiangsu Province (2017-GDZB-006, Class A), the Natural Science Foundation of Jiangsu Province (BK20181274), the Scientific Research Foundation of Graduate School of Southeast University (YBPY1703), the Open Research Fund of Jiangsu Key Laboratory for Design and Manufacture of Micro-Nano Biomedical Instruments, Southeast University (KF201806), the Scientific Research Fund of Nanjing Institute of Technology (YKJ201859), the Tribo1ogy Science Fund of State Key Laboratory of Tribology (SKLTKF15A11), Open Research Fund of State Key Laboratory of High Performance Complex Manufacturing, Central South University (Kfkt2016-11), Open Research Fund of State Key Laboratory of Fire Science (HZ2017-KF05) and Open Research Fund of State Key Laboratory of Solid Lubrication (LSL-1607).

Author contributions Liu L proposed the topic and outline of the manuscript. Huang Y collected the related information and wrote the manuscript.

Conflict of interest The authors declare no conflict of interest.

Yazhou Huang received his PhD degree from the School of Mechanical Engineering at Southeast University of China in 2018. He joined Nanjing Institute of Technology as a lecturer in 2018. His research interest is mainly focused on the synthesis of nanomaterials for electronic device applications.

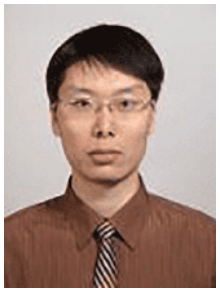

Lei Liu is a Professor of the School of Mechanical Engineering at Southeast University. He is a Distinguished Young Scholar of the National Science Foundation of Jiangsu Province, Excellent Young Scholar of the National Science Foundation of China. He received his PhD degree from the University of Science and Technology of China in 2007. His current research interest focuses on the nanomaterials and devices for medical detection.

原子层沉积二硫化钼的研究进展

黄亚洲[1,2], 刘磊[2*]

摘要 作为一种特殊的化学气相沉积技术, 原子层沉积在薄膜制造领域得到广泛的应用. 得益于自限制化学反应, 原子层沉积所制备的薄膜具有优异的均匀性且精确可控. 基于原子层沉积技术, 在复杂、大面积基底上制备的薄膜厚度可以控制在原子尺度精度(0.1 nm). 因此, 它已经被用来制备二维MoS_2材料. 本综述首先介绍了原子层沉积MoS_2薄膜的相关研究进展, 然后就前驱体、衬底、温度和退火等工艺参数对薄膜质量的影响进行了分析, 最后对原子层沉积制备的MoS_2在电化学催化领域的应用进行了评论. 该综述不仅回顾了原子层沉积MoS_2的研究进展, 而且指出了尚存的挑战和突破的希望.

